Marine Geology 275 (2010) 53–65

Contents lists available at ScienceDirect

Marine Geology

journal homepage: www.elsevier.com/locate/margeo

Morpho-acoustic variability of cold seeps on the continental slope offshore Nicaragua: Result of fluid flow interaction with sedimentary processes

Dietmar Buerk [a,*], Ingo Klaucke [b], Heiko Sahling [c], Wilhelm Weinrebe [b]

[a] IFM-GEOMAR/SFB 574, Wischhofstrasse 1-3, 24148 Kiel, Germany
[b] IFM-GEOMAR Leibniz Institute of Marine Sciences, Wischhofstrasse 1-3, 24148 Kiel, Germany
[c] MARUM — Center for Marine Environmental Sciences and Faculty of Geosciences, University of Bremen, Klagenfurter Straße, 28359 Bremen, Germany

ARTICLE INFO

Article history:
Received 18 November 2009
Received in revised form 7 April 2010
Accepted 27 April 2010
Available online 7 May 2010

Communicated by D.J.W. Piper

Keywords:
mound structures
cold seeps
fluid venting
sedimentation
erosion
sidescan sonar
Nicaragua

ABSTRACT

Based on multibeam bathymetry, high-resolution deep-towed sidescan sonar and Chirp subbottom profiling 32 cold seep sites, already identified in Sahling et al. (2008a), have been studied in an approximately 1000 km^2 large area ranging from 800 to 2600 m water depth along the middle slope of the active continental margin offshore Nicaragua. Ground truthing is available from towed camera surveys and coring on seven of the structures. The seeps occur in different settings on the slope: upslope and along the headwall of large submarine slides, as isolated eroded massifs, and forming linear ridges between deeply incised canyons. The seep sites show a wide range regarding their size and morphology, their backscatter intensity patterns, their structure in subbottom profiles, and their fluid venting activity inferred from seafloor observations. Surface extension of the seep sites ranges from less than 200 to more than 1500 m in diameter, and relief height varies between no relief and 180 m. Indications of extruded materials such as mud flows are not observed in the area of the seep sites. Instead the seeps are characterized by high proportions of authigenic carbonates. The carbonates occur as crusts, detritus, or single layers embedded in the seafloor sediments. They appear as high backscatter intensities on sidescan sonar images. On some seep sites living vent fauna indicative of active seepage is observed, but gas bubbles have not been observed. To explain the high morphological variability of the features, we propose a generic model including the interaction of several processes: (1) episodic fluid venting and associated authigenic carbonate formation; (2) background sedimentation and subsidence; (3) linear erosion along canyons and denudation on the slope surface.

1. Introduction

Cold seeps are areas of the seafloor where cold, methane-rich fluids emanate and create the basis for distinct depositional environments and benthic communities (Paull et al., 1984). Cold seeps are well identified and imaged with geoacoustic data by either gas bubble streams (so-called "flares") in single-beam echosounder profiles (Obzhirov et al., 1989; Heeschen et al., 2003; Egorov et al., 2003), or high backscatter intensities on sidescan sonar images (Henry et al., 1990; Johnson et al., 2003; Sager et al., 2004) and multibeam bathymetry data (Orange et al., 2002; Jerosch et al., 2007). The Pacific continental margin offshore Central America shows a large number of cold seeps associated with faults, slump scars of submarine landslides, areas without morphological expression (backscatter anomalies) and mounds (Sahling et al., 2008a). Mounds in this sense are seafloor features of several hundred metres width and with positive relief of generally less than 100 m. They are the result of cold seep activity. These mounds are particularly abundant offshore Nicaragua and Northern Costa Rica (Fig. 1; Sahling et al., 2008a). They differ from mud volcanoes that have similar dimensions and morphology in that they do not show signs of sediment mobilisation and the expulsion of mud breccia (Klaucke et al., 2008). Klaucke et al. (2008) attributed the absence of mud volcanism offshore Central America to the tectonic regime at this erosive active margin, but did not explain the mechanisms of the formation and evolution of these mounds.

High-resolution geoacoustic data complemented with video observations and coring offshore Nicaragua show a great variety in morphology, backscatter intensity patterns and dimension of cold seeps. In the present paper, based on these observations a conceptual generic model of cold seeps has been developed. This model explains the observed variability of cold seeps by the interplay of three factors: the intensity of fluid escape, the rate of sedimentation, and the rate of erosion on the continental slope. Varying degrees of intensity and preponderance of each of these processes result in quite different seafloor expressions of cold seeps.

* Corresponding author. Now at GKSS Research Centre, Institute of Coastal Research, Max-Planck-Str. 1, 21502 Geesthacht, Germany. Tel.: +49 4152 87 1535; fax: +49 4152 87 1525.
E-mail address: Dietmar.Buerk@gkss.de (D. Buerk).

0025-3227/$ – see front matter © 2010 Elsevier B.V. All rights reserved.
doi:10.1016/j.margeo.2010.04.007

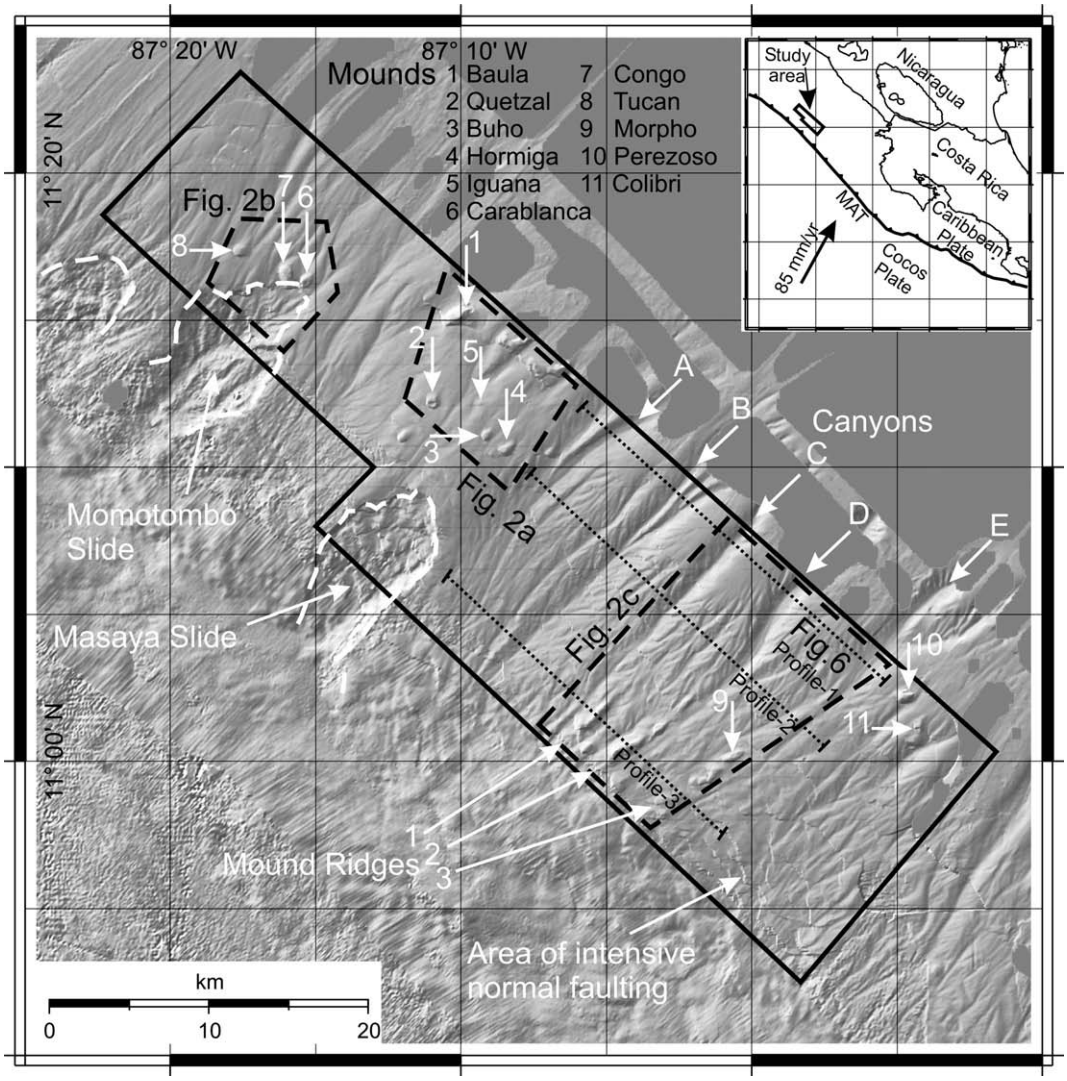

Fig. 1. Shaded relief map of the study area offshore Nicaragua showing the main morphological features: mounds, slides and canyons. Dashed lines denote approximate extension of sidescan sonar drapes shown in Fig. 2, dotted lines represent location of cross-sections in Fig. 6. The box marks the area of the high-resolution sidescan sonar survey. MAT: Middle America Trench.

2. Geological setting and previous work

The study area offshore Nicaragua is part of the erosive Central American convergent margin, where oceanic crust of the Cocos Plate, formed at the East Pacific Rise (EPR), subducts at a rate of 85 mm per year under the Caribbean Plate (Fig. 1, inset; von Huene et al., 2000; Barckhausen et al., 2001; DeMets, 2001; Ranero et al., 2003). Recent seismic cross-sections from Costa Rica to Nicaragua indicate that tectonic erosion is active along most of the Middle America convergent margin (McIntosh et al., 2007), which results in extensional tectonics at the continental slope (Meschede et al., 1999). Offshore Nicaragua, the continental slope is 55 km wide and can be divided into a gently dipping upper slope (2.5°) with an approximately 1500 m thick sediment cover, a narrow middle slope, steepening to 17° dip angle and with a sediment cover of less than 1000 m, and a lower slope dipping 6° and with a thin sediment cover of 500 m (Ranero et al., 2000). Sediment accumulation rates, derived from the correlation of dated tephra layers in marine cores from the continental slope offshore Nicaragua reveal strong lateral and temporal variations (Kutterolf et al., 2008a). Deviations from the normal sedimentation rate of 30–40 cm/ka are explained by increased turbidity current activity on the slope, probably linked to erosive phases on land. The slope sediments overlie a rough surface of ophiolitic basement rocks (Flueh et al., 2000; Walther et al., 2000). At the foot of the slope a small frontal prism, consisting mainly of reworked slope sediments, has developed (von Huene et al., 2000). The incoming oceanic plate is covered with approximately 250–300 m of siliceous hemipelagic sediments overlying pelagic calcarous ooze (von Huene et al., 2000), and shows a high seamount density (Berhorst, 2006).

Widespread fluid expulsion along the margin off Costa Rica and southern Nicaragua was documented at landslides, deformation features related to seamount subduction, faults, and mounded structures on the middle slope (Bohrmann et al., 2002; Hühnerbach et al.,

Fig. 2. Sidescan sonar mosaics draped over Digital Elevation Model (DEM) of the seafloor. Extent of mosaics is indicated in Fig. 1, lines across mounds represent position of subbottom profiles shown in Fig. 5. (A) Mounds Quetzal, Buho and Hormiga have circular to elliptical bases and dome-like shapes with smooth upslope and steep downslope flanks. Iguana seep is located on a canyon shoulder and shows very little topographic expression but an irregular outline. The mounds of the Baula Massif (numbered I–V) are situated upslope of an escarpment (dashed line). Mound Baula I is the largest mound discovered with a base of 2150 × 1630 m and a height of up to 180 m. Suspected slumping on Mound Baula I flank is indicated. (B) Mound structures along Momotombo Slide headwall. Gullies are deflected by mounds (indicated by arrows), and discharge over the headwall into slide area. (C) Area of the 3 mound ridges with location of cross-section on Mound Ridge 1 (Fig. 5A).

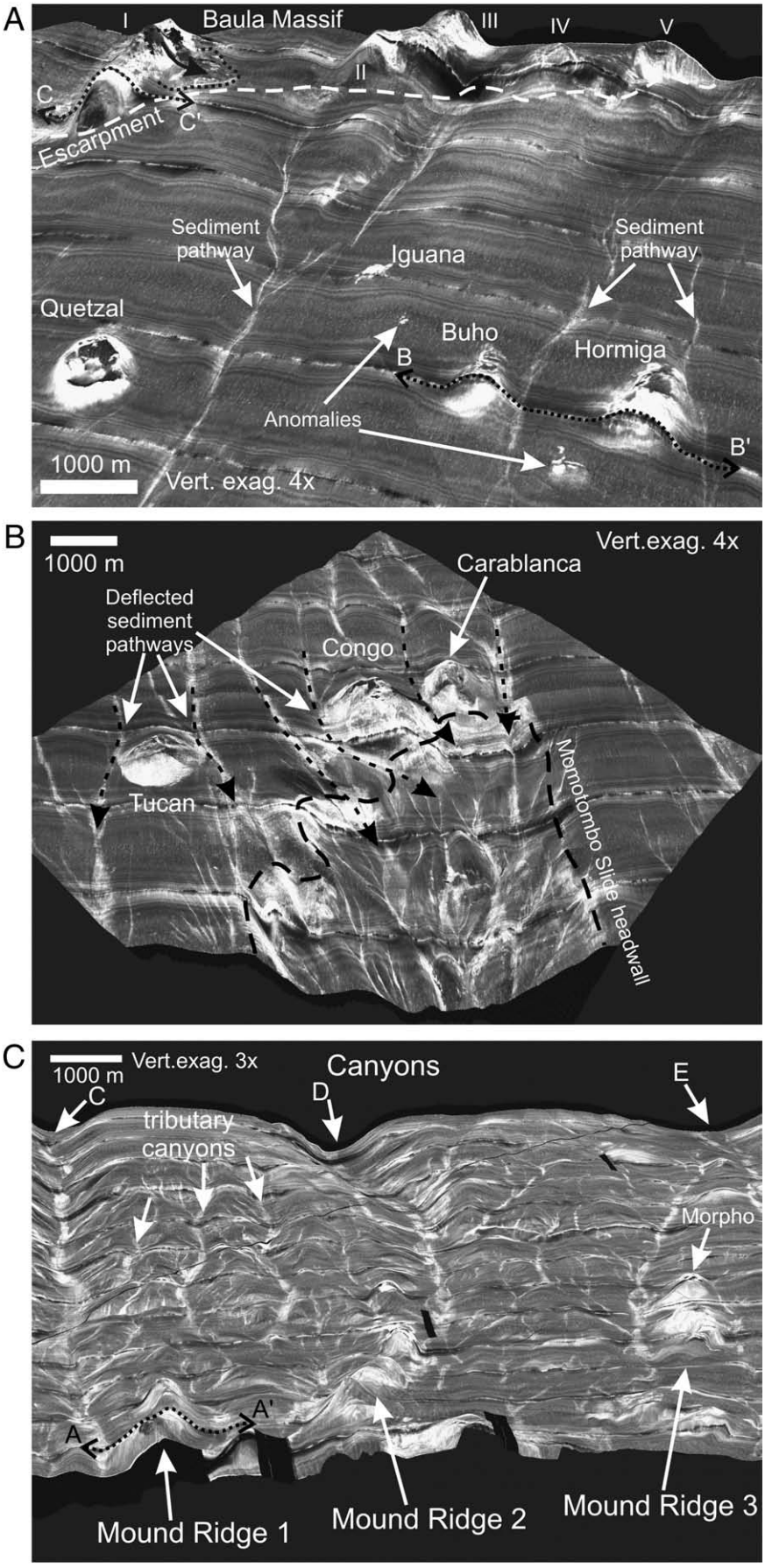
A
Baula Massif
I
II
III
IV
V
C
C'
Escarpment
Sediment pathway
Iguana
Sediment pathway
Quetzal
Buho
Hormiga
B
Anomalies
B'
1000 m
Vert. exag. 4x
B
1000 m
Vert.exag. 4x
Carablanca
Deflected sediment pathways
Congo
Tucan
Momotombo Slide headwall
C
1000 m
Vert.exag. 3x
Canyons
C
D
E
tributary canyons
Morpho
A
A'
Mound Ridge 1
Mound Ridge 2
Mound Ridge 3

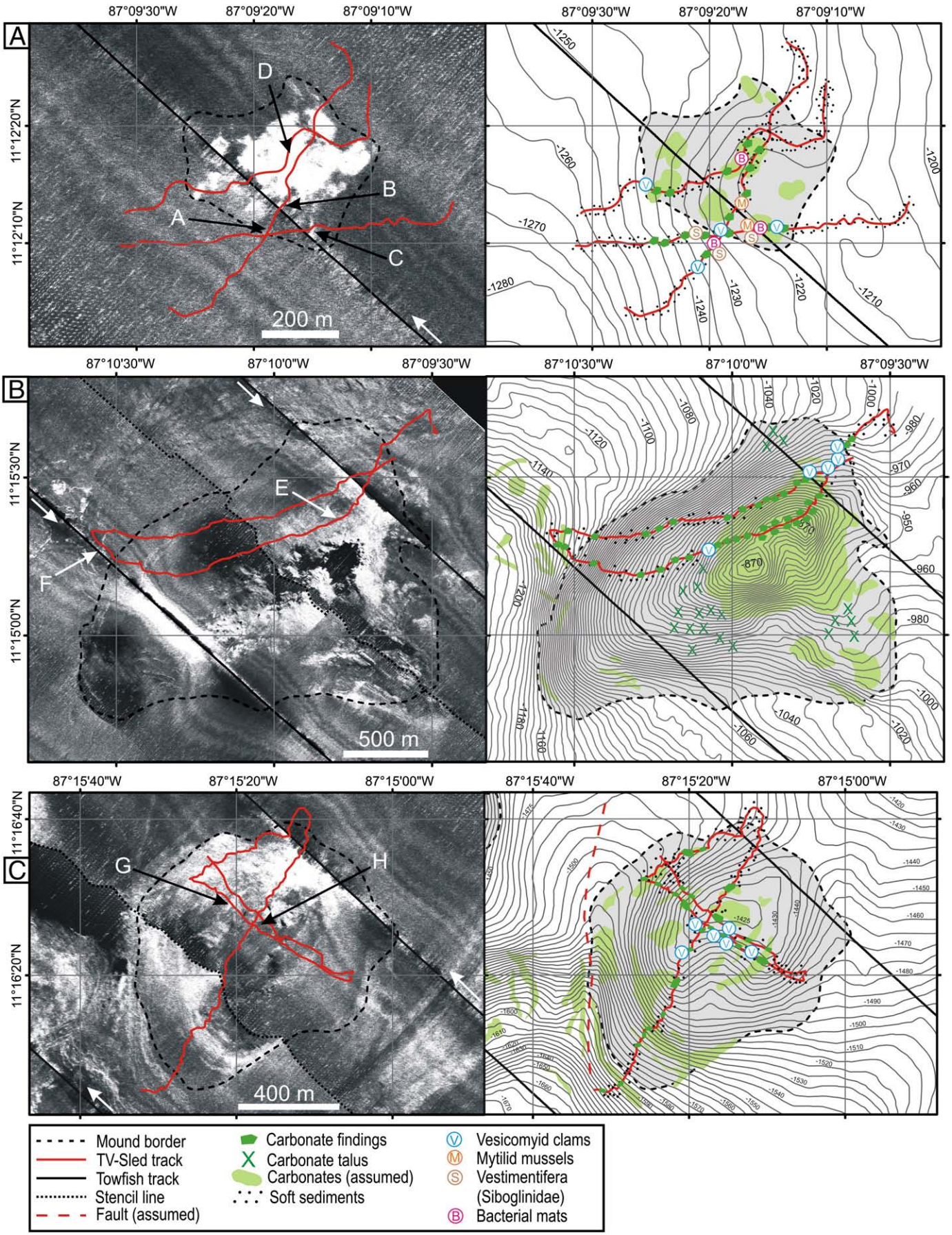

Fig. 3. Sidescan sonar map of Iguana seep (A), Mound Baula I (B) and Mound Carablanca (C) with location of towed camera transects, and interpretation based on seafloor observations and backscatter facies. Letters (A–H) mark positions of seafloor pictures shown in Fig. 4.

2005; Sahling et al., 2008a). These seep sites are not evenly distributed along the slope but occur as a band along the middle slope at 17–40 km landward from the trench (Sahling et al., 2008a). The released fluids contain high concentrations of CH_4 and H_2S (Hensen et al., 2004). In many parts of the margin, widespread and well-developed bottom-simulating reflectors (BSRs) have been documented (Pecher et al., 1998; Talukder et al., 2007), indicating the presence of free gas at the base of the gas hydrate stability zone. Geochemical and isotopic analysis of pore waters from sediment cores on a fluid venting site off Costa Rica (i.e. to the south of the study area) indicates a deep source of the fluids, which are attributed to clay-mineral dehydration within the subducted sediments and thermogenic methane formation (Hensen et al., 2004).

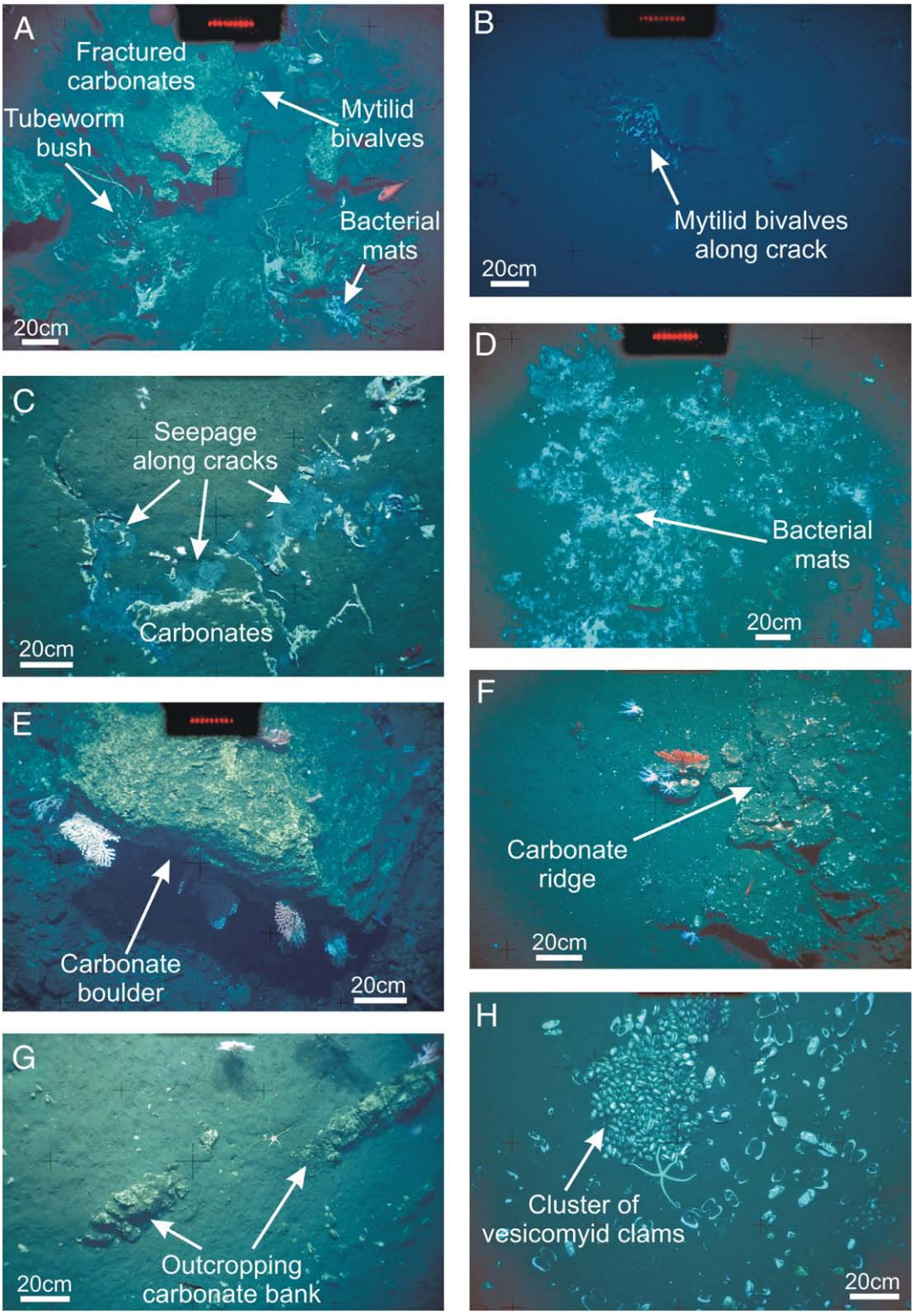

Fig. 4. Images of the seafloor taken by TV-sled at Iguana seep site (A–D), Mound Baula (E–F) and Carablanca (G–H). (A) Fractured carbonates, bush of vestimentiferan tubeworms, small patch of bacterial mats. (B) Small cluster of mytilid bivalves. (C) Seepage along cracks in carbonate crust. (D) Bacterial mats. (E) Large carbonate block. (F) Carbonate ridge sticking out of seafloor sediment. (G) Carbonate bank sticking out of seafloor sediment. (H) Cluster of living vesicomyid clams and scattered clam shells.

The upward migration of the fluids occurs along deep-seated normal faults that would reach down to the plate boundary (Shipley et al., 1990; Ranero and von Huene, 2000; Hensen et al., 2004). Seep structures are believed to follow underlying faults that act as conduits for the fluids (Sahling et al., 2008a). Geochemical measurements and modeling indicate that fluid flow rates are in the order of cm per year and variable in space and time (Hensen et al., 2004; Hensen and Wallmann, 2005; Mau et al., 2006, 2007). The highest fluid-expulsion rates have been estimated by methane concentrations in the water column along major slump scars related to seamount subduction (Mau et al., 2007). However, these flow rates are much lower than those measured at accretionary active margins such as Hydrate Ridge (Torres et al., 2002) or New Zealand (Linke et al., 2009). U/Th dating of authigenic carbonates from mound structures offshore Nicaragua (Kutterolf et al., 2008b) and comparison with ages of mounds offshore Costa Rica (Petersen et al., 2009) suggest ages in the order of several thousand to tens of thousands of years for the seeps offshore Nicaragua.

3. Data and methods

Analysis and interpretation of fluid venting sites offshore Nicaragua are based on combined bathymetric, sidescan sonar, seafloor video and coring data, obtained during *RV SONNE* cruise SO173 (July–September 2003) to the Pacific margin of Costa Rica and Nicaragua (Flueh et al., 2004).

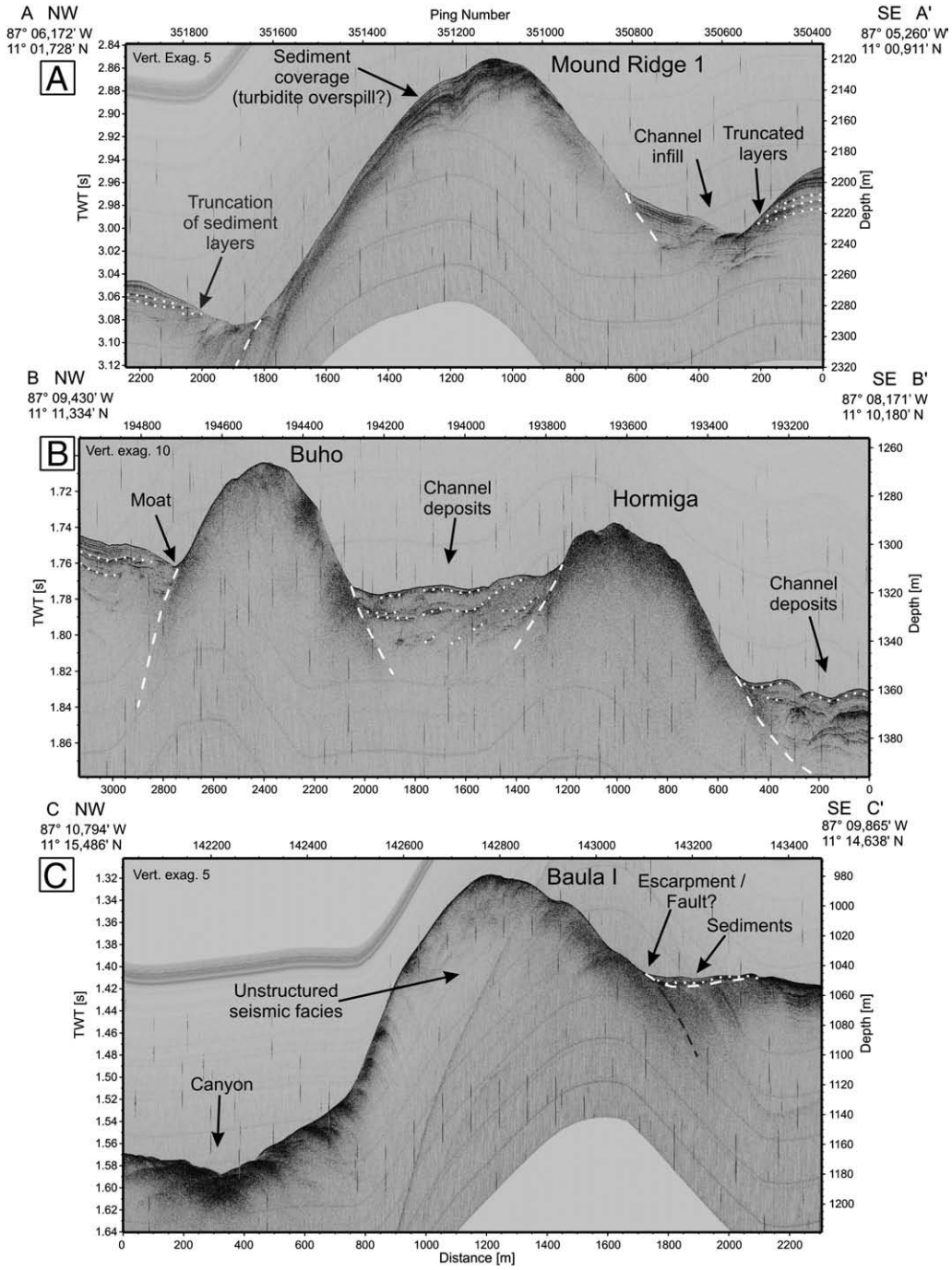

Fig. 5. Subbottom profiles across Mound Ridge 1 (A), Mound Buho and Mound Hormiga (B), and Mound Baula I (C). For location of profiles see Fig. 2A and C. Dashed lines indicate border of seeps, dotted lines mark sediment layers.

Bathymetric data were obtained with the hull-mounted Kongsberg EM120, operating with successive, frequency-coded acoustic signals from 11.25 to 12.60 kHz. The system provides depth and amplitude measurements of 191 beams. A narrow swath width in combination with a ship speed of 3 knots resulted in good data quality and multiple oversampling. The $2\times2°$ beam angle gives a footprint diameter of 28 m at 800 m water depth and 90 m at 2600 m water depth. Depth-sounding measurements were processed with the software package CARAIBES from IFREMER using a statistical approach of iterative gridding with a final grid cell size of 50 m. The grid was then merged with surrounding data from earlier surveys that have lower horizontal resolution (Fig. 1).

Sidescan sonar data were acquired with the digital, deep-towed DTS-1 system operated by IFM-GEOMAR. The DTS-1 is a modified EdgeTech dual-frequency chirp system working with 75 and 410 kHz centre frequencies for a maximum range of 750 and 150 m, respectively. The low frequency mode used during this survey has a maximum across-track resolution of 5.6 cm. A ping repetition rate of 0.98 Hz (or 1.020 s interval) at towing speeds of 2.5–3.0 knots enables an along-track resolution of 1.3–1.5 m. The data have been processed for a pixel size of 1.0 m using the PRISM package (Le Bas et al., 1995). The 75 kHz signal should show only little volume backscatter (Mitchell, 1993) but surface sediments with little backscatter reflectivity allow imaging of slightly buried structures (Klaucke et al., 2008). The EdgeTech Chirp subbottom profiler that is included in the DTS-1 was operated with a 20 ms long pulse at 2–10 kHz. The vertical resolution is in the order of 40 cm and the sediment penetration reaches up to 40 m depending on seabed conditions. The profiler data were corrected for varying water depth of the towfish, using the Seismic Unix package (Stockwell, 1999). Profiles are plotted with a linear distance scale, assuming a constant velocity between profile endpoints.

Eight long (60 km) and 5 short (35 km) slope-parallel 75 kHz sidescan profiles were collected, covering a total of 980 km^2 at the middle continental slope in a water depth ranging from 800 to 2600 m. Navigation of the towfish is based on ship position and cable length using a layback method that integrates towing speed. Ultra-short baseline (USBL) navigation was available for some of the profiles and did not show major discrepancies with towfish navigation based on cable length. The integration of the sidescan sonar mosaic with the (D-GPS positioned) bathymetry and reflectivity data shows a very good match. Presentation of the backscatter data is in normal mode, i.e. high backscatter values are shown in bright tones.

Ground truthing of the geoacoustic data was possible through towed video observations, gravity coring and geochemical sampling with multi-corer on seven of the seep sites during a later leg of the cruise (Flueh et al., 2004). Interpretation of the sidescan images is based on the backscattering facies combined with detailed analysis of the video profiles. Navigation of the video sled was obtained using a short baseline system that provides an accuracy in the range of 1% of the water depth. The possible mismatch between sidescan sonar and video data has been estimated at 10 to 15 m.

4. Seep structures offshore Nicaragua

4.1. Distribution of seeps

Although seep structures occur all over the study area (Fig. 1) distinct clustering with respect to certain environments and settings such as normal faults, canyons and slide headwalls is obvious. Seeps are found (1) upslope of the Masaya Slide (Quetzal, Buho, Hormiga, Iguana; Fig. 2A) and close to the headwall of the Momotombo Slide (Carablanca, Congo, Tucan; Fig. 2B); (2) on linear, cross-slope trending ridges between deeply incised canyons (e.g. Morpho; Fig. 2C); and (3) at shallow depth forming isolated massifs (Baula, Perezoso). Mound Perezoso and Mound Colibri are situated upslope of

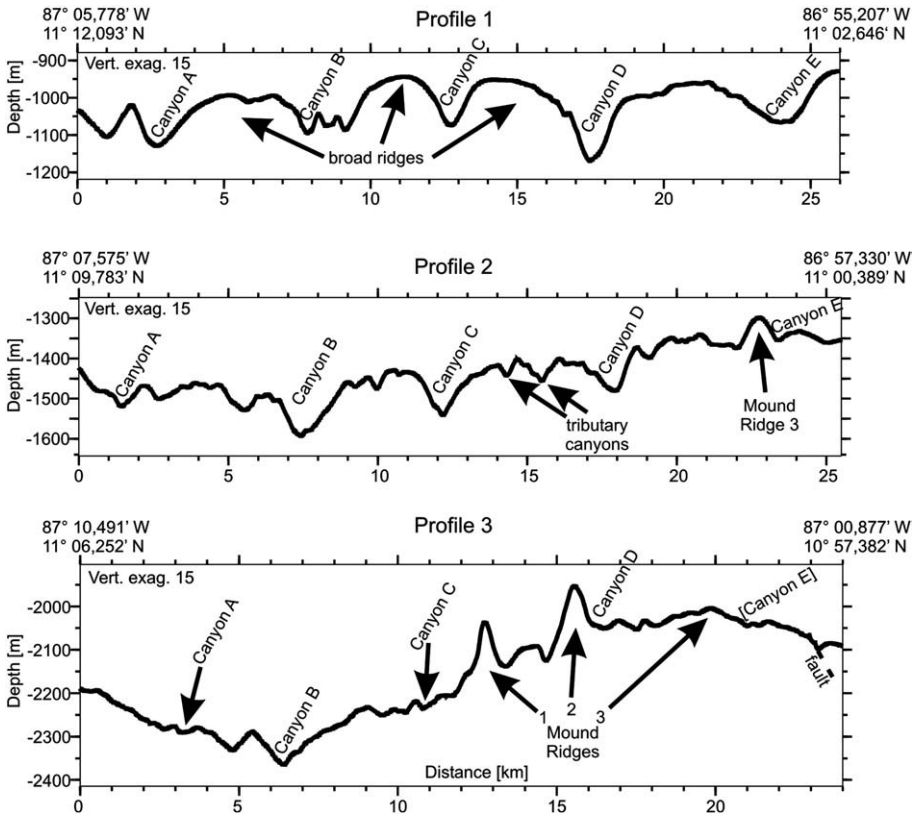

Fig. 6. Topographic cross-sections through canyon area at different water depths (for location see Fig. 1). Note the dissection of the inter-canyon divides by tributary canyons and the erosion of the divides, leaving back the more resistant mound ridges (e.g. between canyon C and D).

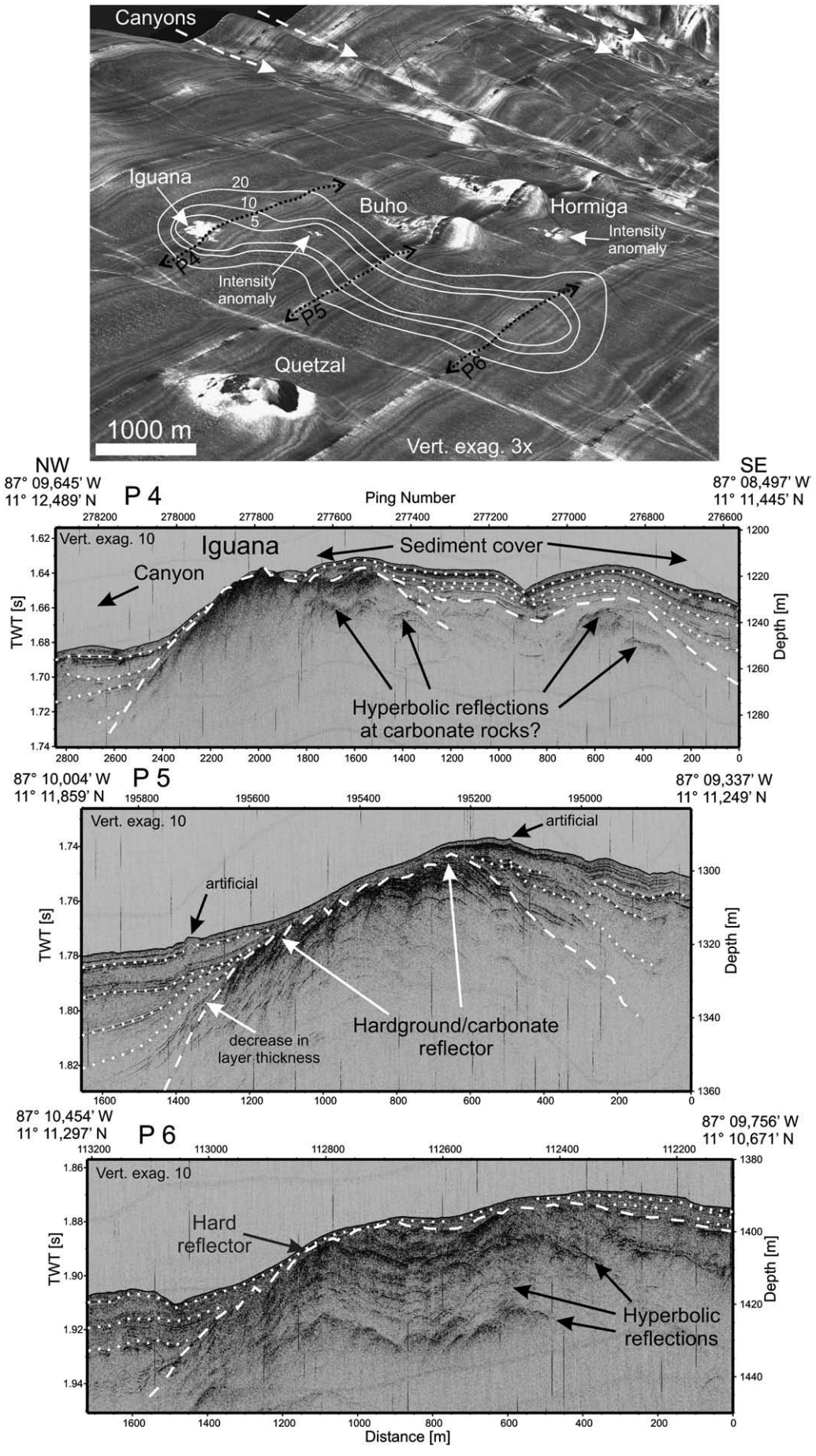
Canyons
Iguana
20
10
5
Buho
Hormiga
Intensity anomaly
P4
Intensity anomaly
P5
P6
Quetzal
1000 m
Vert. exag. 3x
NW
87° 09,645' W
11° 12,489' N
P 4
Ping Number
SE
87° 08,497' W
11° 11,445' N
Vert. exag. 10
Iguana
Canyon
Sediment cover
Hyperbolic reflections at carbonate rocks?
TWT [s]
Depth [m]
87° 10,004' W
11° 11,859' N
P 5
87° 09,337' W
11° 11,249' N
Vert. exag. 10
artificial
artificial
Hardground/carbonate reflector
decrease in layer thickness
TWT [s]
Depth [m]
87° 10,454' W
11° 11,297' N
P 6
87° 09,756' W
11° 10,671' N
Vert. exag. 10
Hard reflector
Hyperbolic reflections
TWT [s]
Depth [m]
Distance [m]

a part of the slope that is affected by intensive normal faulting. The morphological relief of the normal faults is up to 40 m.

4.2. Surface expression of seeps

The seep structures show a large variability with respect to size, morphology, backscatter intensity pattern, and fluid venting activity inferred from seafloor observations (Fig. 2A). In size and morphology the seeps cover a wide range: backscatter anomalies with no topographic relief and diameters of below 200 m, small bulges that rise about 20 m above the surrounding seafloor and diameters of around 450 m (Iguana seep site), dome- or knoll-like mound structures with heights of 40–80 m and diameters of 600–1000 m (Mounds Quetzal, Buho, Hormiga), and, at shallower depth, large structures with steep morphologies, heights of up to 180 m and diameters of more than 2000 m (Mounds Baula I, Perezoso). Mound Baula I belongs to a group of mounds, which form the Baula Massif, located in 800–900 m water depth above an escarpment. They show similar morphologies and backscatter facies. The Mounds Baula II, IV and V are located at the escarpment where indications for slumping and sediment creeping are observed on the sidescan sonar image. On some mounds central depressions may represent slump scars (Mounds Quetzal, Baula I, Carablanca).

All seep sites are characterized by an increased backscatter in reference to the surrounding seafloor. But patterns in sidescan sonar images range from very bright and uniform backscatter signals with very sharp and irregular borders to the surrounding background amplitude values (backscatter anomalies, Iguana seep site; Figs. 2A and 3A) to patchy and mottled backscatter signatures with abundant areas of acoustic shadow (Mounds Quetzal, Buho, Hormiga, Baula I; Fig. 3B). Camera observations suggest that the bright and uniform backscatter corresponds to authigenic carbonates. Living chemosynthetic vent fauna (vesicomyid clams, mytilid bivalves, siboglinid tubeworms and filamentous mats of bacteria), indicative for active seepage (Sibuet and Olu, 1998), is observed in several centres on Iguana seep site (Fig. 3A). Along its southern and southwestern border the high amplitude values in the sidescan sonar image correlate with fractured authigenic carbonates on the seafloor (Fig. 4, A), several occurrences of vent fauna (Fig. 4, B), and hints for active seepage along cracks and fractures in massive carbonates (Fig. 4, C). Along the north and northeast of the seep, hemipelagic sediment with only little carbonate detritus is observed on the seafloor. Here the high backscatter return observed in the sonar image most likely results from a hard reflector at very shallow depth, as seen elsewhere in DTS-1 data (Klaucke et al., 2008). A patch of bacterial mats in the seep centre indicates a high rate of seep activity (Fig. 4, D). Camera observations on other mounds (Mounds Quetzal, Buho, Hormiga, Carablanca and Baula I; Fig. 3) suggest that the patchy and mottled backscatter signature results from fractured carbonates or carbonate blocks of 1.0–1.5 m size. The upslope flanks are often covered with soft sediments while on the other flanks abundant carbonate detritus can be found. Vent fauna (mainly clams) is present, but preferably on soft sediment ponded between the fractured carbonates (Fig. 4, H). On Mound Baula I extensive carbonate pavement, sometimes fractured, forming blocks several metres thick, is observed in the top area (Fig. 4, e). Rare occurrences of vesicomyid clam clusters, approximately 1–2 m across, indicate little fluid venting activity, and are mainly limited to the upslope part of the mound, where sediments border the carbonate pavement (Fig. 3B). A high backscatter lineament along the base of Mound Baula correlates to an outcropping carbonate bed of approximately 1 m thickness (Fig. 4, F). A similar and characteristic circular banding of alternating high and low backscatter intensities is observed on Mound Carablanca (Fig. 3C). The bands of high backscatter often correlate with carbonate rocks or carbonate banks outcropping at the seafloor (Fig. 4, G).

The mounds forming the cross-slope trending ridges between 1650 and 2300 m water depth are elongated (Fig. 2C). Their short axis varies between 400 and 800 m and their long axis between 800 and 1200 m. The slope-parallel heights are between 50 and 100 m. The ridges are of different lengths. Mound Ridge 1 is short and consists of only two mounds. Four seep centres form Mound Ridge 2. In its lower part two possible mounds, which are offset from the ridge axis, are only partially covered by the sidescan sonar image. Mound Ridge 3 consists of two possible seep sites in the deeper part and Mound Morpho and an unnamed mound at 1700 and 1800 m water depth, respectively. Upslope on the ridge at 1190 m, a patch of high backscatter with little topographic relief may mark another seep site. Several subbottom profiles crossing the mound ridges and their neighbouring canyons show truncated sediment layers, but also deposition of overbank deposits on the shoulders of the canyons or in higher parts on the mounds themselves (Fig. 5A). Trench-parallel topographic cross-sections in different water depths of the slope through the canyon area show the incision of the canyons into the slope morphology (Fig. 6). In the uppermost cross-section the broad ridges between the canyons have a smooth surface (Profile 1). The cross-section at intermediate depth reveals that tributary canyons cut into the inter-canyon divides leading to a rough surface superimposed on the broad ridges (Profile 2). In the lowermost cross-section (Profile 3) the broad inter-canyon divides are no longer visible (e.g. between canyon B and C). However, in certain cases distinct, narrow ridges between the canyons remain present (e.g. between canyon C and D). The absence of inter-canyon divides at this water depth can be explained by either erosion of the divides or reduced incision of the canyons. The presence of tributary canyons at mid-slope (Profile 2) indicates the former to be more likely.

4.3. Buried seeps and subsurface continuity of the seep structures

Subbottom profiles across the seeps evidence sediment deposition, erosion and fluid venting processes and allow the subsurface continuity of the structures to be estimated. Sediment coverage of a seep can result from overspill deposits (Fig. 5A), or is imaged as a hemipelagic drape on the seep-affected seafloor (Fig. 7, P4). Chaotic channel deposits or canyons showing truncated sediment layers often border the mounds (Fig. 5A,B). Sometimes a moat has developed (Fig. 5B). The unstructured seismic facies below the seep sites could result from low signal penetration due to strong diffusive surface reflection (Fig. 5C).

Buried, extinct seeps are even more widespread as evidenced beneath the Iguana seep and two profiles further downslope (i.e. to the NW of Mound Buho). In these profiles (Fig. 7) unstructured seismic facies with some arcuate shaped reflections is covered to a large degree with layered slope sediments. Onlapping sediment layers decreasing in layer thickness are observed along the middle profile. The layers terminate against the approximately 800 m wide structure. A high-reflectivity horizon, reaching up to 2.5 m below the seafloor, marks the top of the structure. A hemipelagic drape, thick enough to prevent an intensity anomaly in the sidescan sonar data, covers the reflector. Due to the decrease in layer thickness, the termination of layers, and the absence of flares or free gas in the water column, we interpret this reflector as buried hardgrounds, most likely patches of authigenic carbonate formations. The hyperbolic reflections observed deeper in the sub-seafloor would then result from carbonates formed during past seep activity, now buried under younger slope sediments. In the sidescan sonar image only the Iguana seep and another small intensity anomaly can be observed as piercing points of the structure at the seafloor. Interpolation of the depth contours of the structure top

Fig. 7. Sidescan sonar mosaic draped over DEM of the seafloor (top). Contour lines denote estimated depth of strong reflector on top of seep facies in metres below seafloor, based on cross-sections P4, P5 and P6. Future denudation and erosion on the slope will potentially turn this sub-seafloor structure into a mound ridge as shown in Fig. 2C.

reveals an extension of approximately 4500 m across the slope (Fig. 7). We speculate that this buried ridge is similar to ridges exposed further south (Fig. 2C) and that differences relate to degrees of erosion or spill-over deposition from adjoining canyons.

4.4. Generic model explaining seep variability

Different processes such as sediment deposition, fluid venting and authigenic carbonate precipitation, and erosion affect cold seep environments and must be taken into account when explaining cold seep formation. The high variability of the seep structures offshore Nicaragua results from the predominance of one of these processes or from a combination of several of the observed processes, which in turn depends on the location of the seep with respect to sedimentary and erosional processes on the slope. Each seep site is seen as the result of the three interacting processes and can be placed in a ternary diagram with corners representing fluid seepage, sediment deposition and erosion (Fig. 8). Fluid seepage is the key process responsible for changing the seafloor properties. The duration or intensity of the seep activity determines the amount of authigenic carbonate precipitation. However, the morphology of a given seep is to a large degree controlled by sedimentary and erosional processes. A seep site located over a longer period in an erosive environment will be characterized by an absence of a sedimentary coverage. It will develop a steep morphology and its surface will show largely exposed carbonates. If the seep is still active, it will also exhibit vent biota feeding on the methane-rich fluids. An active seep site in an area of the slope with high sediment deposition will be characterized by the presence of layered sediments in the subbottom profiles partially covering the seep location, typical vent fauna indicating active seepage, and strong backscatter in the sidescan sonar image resulting from recently formed carbonates. The hardgrounds can be covered with hemipelagic sediments, overbank deposits of nearby turbidity currents, or debris flows pouring onto the seep site. But as long as the seepage continues the typical features like authigenic carbonates or vent biota will form or settle close to its surface. When seep activity ceases the site will be drowned under sediment deposits.

Mound Baula shows a clearly erosion-dominated morphology (Figs. 2A, 5C, and 8). The extensive carbonate pavement and the absence of dense vent biota indicate a long-lasting or vigorous but now ceased activity. Mound Buho and Mound Hormiga (Figs. 2A and 5B) are seep sites where all three processes interact with similar intensity (Fig. 8). Erosion or surface abrasion resulted in a morphology arising above the surrounding seafloor, seep activity is moderate but present, and the upslope flanks are smooth due to sediment coverage. Neighbouring channel deposits indicate sediment bypass from upslope. Mound Iguana represents a highly active seep site located in an environment with high sediment deposition rates, as indicated by the sediment coverage and the dense clusters of vent biota (Figs. 2A, 3A, and 7).

5. Discussion

Our model accounting for the observed variability of cold seeps offshore Nicaragua relies on the interaction of focused fluid flow with sedimentation and erosion on the continental slope. These processes vary in intensity in space and time and the possible amplitude of these variations needs to be discussed and possibly constrained. In addition, the nature of the cold seeps offshore Nicaragua needs some clarification.

5.1. Nature of the seeps

Mound structures offshore Central America have often been described as mud volcanoes, mud mounds or mud diapirs, based on their morphology, geochemical measurements or seismic profiles (Grevemeyer et al., 2004; Mau et al., 2006; Moerz et al., 2005; Talukder et al., 2007). It has been neglected that the escape of cold, methane-rich fluids and their anaerobic oxidation form depositional environments which can, in combination with surface processes, result in structures with similar morphology and characteristics, but without the need of large-scale sediment mobilisation. Authigenic carbonate precipitation consolidates slope sediments and provides a framework for trapping more of the downslope sediment transport than areas without seeps. In combination with erosional processes, which vary in intensity on the steep middle slope, this accounts for the observed morphologies. The mounds offshore Central America are most likely recent equivalents of ancient seep carbonate massifs such as those described from New Zealand (Campbell et al., 2008).

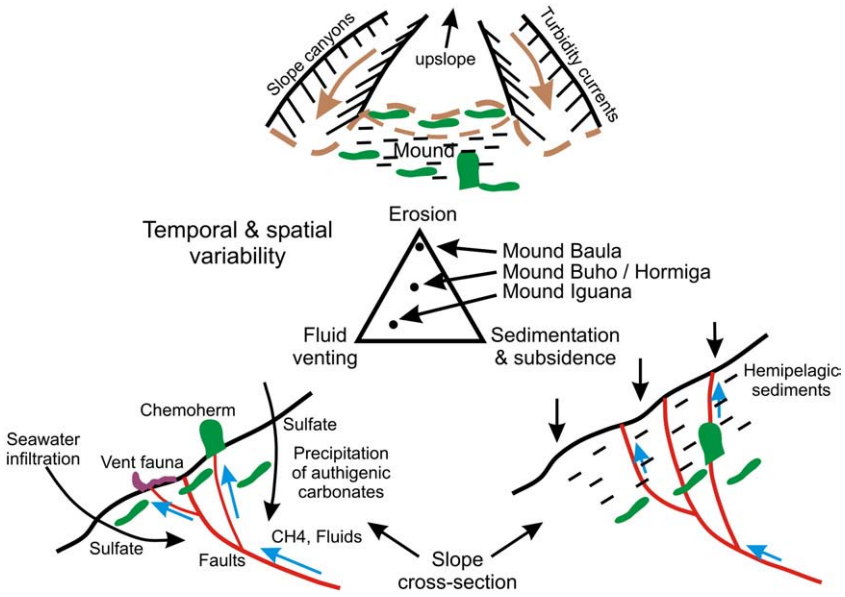

Fig. 8. Generic model explaining seep variability including several, temporally and spatially variable, interacting processes: seepage of methane-rich fluids lead to precipitation of authigenic carbonates (below seafloor or above seafloor as chemoherms; lower left). In times of low seep activity or when sedimentation rate increases locally, deposition of hemipelagic sediments and subsidence dominate (lower right). Erosion by turbidity currents or debris flows along submarine canyons may shape the slope surface according to its resistance against erosion (top). Dots inside triangle indicate location of three seep sites with respect to slope processes.

5.2. Rates, variability, and interaction of processes

5.2.1. Fluid venting

Estimates of fluid flow rates and methane output for the seeps along the Central American margin are mainly based on measurements from offshore Costa Rica (Mau et al., 2006; Hensen and Wallmann, 2005). Emission of methane as free gas in the water column was not observed in raw sidescan sonar swaths or echosounder profiles. It can be assumed that, similar to Costa Rica, the methane is mainly transported dissolved in the vent fluids. Methane supply consequently depends on fluid advection rates and methane concentration of the fluid. The composition of the chemosynthetic communities found on a seep site has been used as a proxy for seep activity (Mau et al., 2006; Sahling et al., 2002, 2008b). Following this approach recent fluid flow rates offshore Nicaragua are probably low compared to rates observed offshore Costa Rica. The prevalent seep biota are vesicomyid clams and clamshells. Significant numbers of bacterial mats, mytilid bivalves and vestimentiferan tubeworms have been found only at the Iguana seep site. The lack of high numbers of chemosynthetic fauna on many seeps and the predominance of carbonate precipitates however could indicate a long-lasting, but now decreased seep activity (Sager et al., 2003). Rates of carbonate crust formation associated with the fluid venting are not known offshore Nicaragua. Luff and Wallmann (2003) derived values of 1 m per 20,000 years or 50 mm/ka of carbonate precipitation for a core from Hydrate Ridge.

Temporal variations in the seep activity (and hence methane supply) are reported in several studies, and are attributed to earthquake activity and seismotectonic processes (Mau et al., 2007; Brown et al., 2005) or eustatic sealevel changes with higher flow rates at low sealevel (Teichert et al., 2003). Besides external triggering through seismotectonic activity or sealevel changes, fluid flow rates can be variable due to self-induced changes in permeability, as was shown in numerical simulations of carbonate precipitation and dissolution rates with data from Hydrate Ridge (Luff et al., 2005). The simulation predicted cycles of carbonate crust formation and dissolution with a duration of 2000–2700 years, and resulted in several distinct carbonate layers. Such temporal variations in fluid flow rates might be reflected in the carbonate beds observed on Mound Baula and Mound Carablanca (Figs. 3B,C and 4F,G).

5.2.2. Sedimentation

Sedimentation rates offshore Nicaragua, as for the entire active Central American Margin, are rather low because of limited sediment supply, resulting in a thin sediment cover and subsequent formation of an erosive margin (von Huene et al., 2004). Sediment delivery offshore Nicaragua is mainly controlled by tectonic and climatic processes on the coast and shelf, and result in average sedimentation rates of 30–40 cm/ka on the continental slope (Kutterolf et al., 2008a). There are, however, strong local variations in sedimentation rates. In contrast to Costa Rica where the slope shows some areas of smooth slope topography (Fekete, 2006; Sahling et al., 2008a; Klaucke et al., 2008), intra-slope basins are not present offshore Nicaragua. The narrow and steep continental slope offshore Nicaragua is dissected by canyons which originate at water depths of around 500 m or less and can be traced down to a zone of increased slumping at roughly 2500 m water depth. Spill-over deposition from turbidity currents transiting within the canyons will lead to increased sedimentation on the ridges separating the canyons (Fig. 5A). In addition, the subsidence of the slope, controlled by tectonic erosion at the base of the margin wedge, can lead to seafloor oversteepening (Meschede et al., 1999). This may result in sediment creeping or slumping and the occurrence of debris flows. The location of a seep site on the slope with respect to the various sediment pathways therefore determines whether the site is covered with overbank deposits from nearby turbidity currents, deposits of debris flows, hemipelagic deposits, or even experiences no sediment deposition.

5.2.3. Erosion

Erosion of the continental slope offshore Nicaragua is dominated by canyon incision into slope sediments (Fig. 5A) of the Pliocene–Holocene El Salto Formation (Ranero et al., 2000). Erosion is therefore strongest at the canyon axis and decreases rapidly outside of the canyon, where most likely sedimentation predominates. In addition, erosion rates probably varied over geological times with highest canyon incision rates during falling sealevel. Finally, erosion might be altered by fluid flow and subsequent authigenic carbonate precipitation, which increases sediment strength and resistance to erosion and might ultimately affect the location of downslope sediment pathways. Actual erosion rates offshore Nicaragua are not known. On a similar sediment-starved margin offshore Peru, Kukowski et al. (2008) tried to estimate the incision rates of gullies and derived values between 10 and 33 cm/ka. Erosion rates offshore Nicaragua could be rather high as slopes are steep and capable of generating ignitive turbidity currents (Parker, 1982). On the other hand, sediment supply is limited and turbidity currents are probably rare.

5.3. Cold seeps and slope failure

The close spatial relationship between the Masaya and Momotombo slides and mound fields that are located just upslope of these slides (Fig. 1) suggest a genetic link between rising fluids and landsliding offshore Nicaragua. Fluid flow and changes in fluid flow rates alter pore pressure, which is one of the major factors inducing sediment failure (Hampton et al., 1996). On the other hand, landsliding exposes deeper sediment layers and can lead to lateral fluid seepage along permeable beds, such as reported by Mau et al. (2007). Furthermore, major landsliding offshore Costa Rica is related to the subduction of seamounts (Dominguez et al., 1998; Hühnerbach et al., 2005) that generate updoming and lead to intense faulting of the overriding plate and fluid seepage along these faults (Hühnerbach et al., 2005; Sahling et al., 2008a). Similar faulting is not observed offshore Nicaragua, despite indications for a subducting seamount beneath Masaya slide (Talukder et al., 2008). Instead, alignment of mounds along the headwall of Masaya and, in particular, Momotombo slides suggests that fluid escape triggered sediment failure and not vice-versa. However, additional work is required in order to decipher the history of these large landslides that are old enough for a new drainage pattern to develop within the slide area.

6. Conclusions

Combined multibeam bathymetry and high-resolution sidescan sonar mapping of the continental slope offshore Nicaragua allowed imaging of 32 cold seep sites. They show a wide variety with respect to size, morphology, backscatter intensity pattern, subbottom profile facies, and fluid venting activity, ranging from large and steep mound structures, often capped with extensive pavements of authigenic carbonates, to small backscatter anomalies without significant topographic expression. We explained this variability with a generic model including three interacting processes: fluid venting, sediment accumulation and erosion. Fluid venting with associated authigenic carbonate formation is the primary process and can be variable in time. Sediment accumulation and erosion occur in small lateral distances on the steep slope and can shift rapidly. The preponderance of one process controls the appearance of a given seep site. Mud flows or other sediment mobilisation processes have not been imaged in the geoacoustic data.

Acknowledgements

The crew and scientists of *RV SONNE* cruise SO173 are thanked for their invaluable help at sea. Funding has been provided by the German Ministry of Education and Research (BMBF) and the German Research Foundation (DFG). This publication is contribution no. 190 of the

Sonderforschungsbereich 574 “Volatiles and Fluids in Subduction Zones” at Kiel University. Reviews by Marc De Batist, Douglas G. Masson and an anonymous reviewer are gratefully acknowledged.

References

Barckhausen, U., Ranero, C.R., von Huene, R., Cande, S.C., Roeser, H.A., 2001. Revised tectonic boundaries in the Cocos Plate off Costa Rica: implications for the segmentation of the convergent margin and for plate tectonic models. Journal of Geophysical Research 106 (B9), 19207–19220.

Berhorst, A., 2006. Die Struktur des aktiven Kontinentalhangs vor Nicaragua und Costa Rica — marin-seismische Steil-und Weitwinkelmessungen. Dissertation thesis, 153 pp. Christian-Albrechts-Universität, Kiel, Germany.

Bohrmann, G., Heeschen, K., Jung, C., Weinrebe, W., Baranov, B., Cailleau, B., Heath, R., Hühnerbach, V., Hort, M., Masson, D., Trummer, I., 2002. Widespread fluid expulsion along the seafloor of the Costa Rica convergent margin. Terra Nova 14, 69–79.

Brown, K.M., Tryon, M.D., DeShon, H.R., Dorman, L.M., Schwartz, S.Y., 2005. Correlated transient fluid pulsing and seismic tremor in the Costa Rica subduction zone. Earth and Planetary Science Letters 238 (1–2), 189–203.

Campbell, K.A., Francis, D.A., Collins, M., Gregory, M.R., Nelson, C.S., Greinert, J., Aharon, P., 2008. Hydrocarbon seep-carbonates of a Miocene forearc (East Coast Basin), North Island, New Zealand. Sedimentary Geology 204, 83–105.

DeMets, C., 2001. A new estimate for present-day Cocos-Caribbean plate motion: implications for slip along the Central American volcanic arc. Geophysical Research Letters 28 (21), 4043–4046.

Dominguez, S., Lallemand, S.E., Malavieille, J., von Huene, R., 1998. Upper plate deformation associated with seamount subduction. Tectonophysics 293, 207–224.

Egorov, V.N., Polikarpov, G.G., Gulin, S.B., Artemov, Yu.G., Stokozov, N.A., Kostova, S.K., 2003. Present-day views on the environment-forming and ecological role of the Black Sea methane gas seeps. Marine Ecology Journal 2, 5–26 (in Russian).

Fekete, N., 2006. Dewatering through mud mounds on the continental fore-arc of Costa Rica. Dissertation thesis, 161 pp. Christian-Albrechts-Universität, Kiel, Germany.

Flueh, E.R., Ranero, C., von Huene, R., 2000. The Costa Rican Pacific margin: from accretion to erosion. Zentralblatt für Geologie und Paläontologie 669–678.

Flueh, E., Söding, E., Suess, E. (Eds.), 2004. RV SONNE Cruise Report SO173/1, 3&4 — Subduction II: the Central American Continental Margin. GEOMAR Report, vol. 115. GEOMAR, Kiel.

Grevemeyer, I., Kopf, A., Fekete, N., Kaul, N., Villinger, H.W., Heesemann, M., Wallmann, K., Spieß, V., Gennerich, H.-H., Müller, M., Weinrebe, W., 2004. Fluid flow through active mud dome Mound Culebra offshore Nicoya Peninsula, Costa Rica: evidence from heat flow surveying. Marine Geology 207, 145–157.

Hampton, M.A., Lee, H.J., Locat, J., 1996. Submarine landslides. Reviews of Geophysics 34, 33–59.

Heeschen, K.U., Tréhu, A.M., Collier, R.W., Suess, E., Rehder, G., 2003. Distribution and height of methane bubble plumes on the Cascadia Margin characterized by acoustic imaging. Geophysical Research Letters 30, 1643. doi:10.1029/2003GL016974.

Henry, P., Le Pichon, X., Lallemant, S., Foucher, J.-P., Westbrook, G.K., Hobart, M., 1990. Mud volcano field seaward of the Barbados Accretionary complex: a deep towed sidescan sonar survey. Journal of Geophysical Research 95B, 8917–8929.

Hensen, C., Wallmann, K., 2005. Methane formation at Costa Rica continental margin — constraints for gas hydrate inventories and cross-décollement fluid flow. Earth and Planetary Science Letters 236, 41–60.

Hensen, C., Wallmann, K., Schmidt, M., Ranero, C.R., Suess, E., 2004. Fluid expulsion related to mud extrusion off Costa Rica — a window to the subducting slab. Geology 32, 201–204.

Hühnerbach, V., Masson, D.G., Bohrmann, G., Bull, J.M., Weinrebe, W., 2005. Deformation and submarine landsliding caused by seamount subduction beneath the Costa Rica continental margin — new insights from high-resolution sidescan sonar data. Geological Society, London, Special Publications 244, 195–205.

Jerosch, K., Schlüter, M., Foucher, J.-P., Allais, A.-G., Klages, M., Edy, C., 2007. Spatial distribution of mud flows, chemoautotrophic communities, and biogeochemical habitats at Håkon Mosby Mud Volcano. Marine Geology 243, 1–17.

Johnson, J.E., Goldfinger, C., Suess, E., 2003. Geophysical constraints on the surface distribution of authigenic carbonates across the Hydrate Ridge region, Cascadia margin. Marine Geology 202, 79–120.

Klaucke, I., Masson, D.G., Petersen, C.J., Weinrebe, W., Ranero, C.R., 2008. Multifrequency geoacoustic imaging of fluid escape structures offshore Costa Rica: implications for the quantification of seep processes. Geochemistry Geophysics Geosystems 9, 4. doi:10.1029/2007GC001708.

Kukowski, N., Hampel, A., Hoth, S., Bialas, J., 2008. Morphotectonic and morphometric analysis of the Nazca plate and the adjacent offshore Peruvian continental slope — implications for submarine landscape evolution. Marine Geology 254, 107–120.

Kutterolf, S., Freundt, A., Schacht, U., Bürk, D., Harders, R., Mörz, T., Perez, W., 2008a. Pacific offshore record of plinian arc volcanism in Central America: 3. Application to forearc geology. Geochemistry Geophysics Geosystems 9, 2. doi:10.1029/2007GC001826.

Kutterolf, S., Liebetrau, V., Mörz, T., Freundt, A., Hammerich, T., Garbe-Schönberg, D., 2008b. Lifetime and cyclicity of fluid venting at forearc mound structures determined by tephrostratigraphy and radiometric dating of authigenic carbonates. Geology 36 (9), 707–710.

Le Bas, T.P., Mason, D.C., Millard, N.W., 1995. TOBI image processing — the state of the art. IEEE Journal of Oceanic Engineering 20, 85–93.

Linke, P., Sommer, S., Rovelli, L., McGinnis, D.F., 2010. Physical limitations of dissolved methane fluxes: the role of bottom-boundary layer processes. Marine Geology 272, 209–222. doi:10.1016/j.margeo.2009.03.020.

Luff, R., Wallmann, K., 2003. Fluid flow, methane fluxes, carbonate precipitation and biogeochemical turnover in gas hydrate-bearing sediments at Hydrate Ridge, Cascadia Margin: numerical modeling and mass balances. Geochimica et Cosmochimica Acta 67, 3403–3421.

Luff, R., Greinert, J., Wallmann, K., Klaucke, I., Suess, E., 2005. Simulation of long-term feedbacks from authigenic carbonate crust formation at cold vent sites. Chemical Geology 216, 157–174.

Mau, S., Sahling, H., Rehder, G., Suess, E., Linke, P., Soeding, E., 2006. Estimates of methane output from mud extrusions at the erosive convergent margin off Costa Rica. Marine Geology 225, 129–144.

Mau, S., Rehder, G., Arroyo, I.G., Gossler, J., Suess, E., 2007. Indications of a link between seismotectonics and CH4 release from seeps off Costa Rica. Geochemistry Geophysics Geosystems 8, 4. doi:10.1029/2006GC001326.

McIntosh, K.D., Silver, E.A., Ahmed, I., Berhorst, A., Ranero, C.R., Kelly, R.K., Flueh, E.R., 2007. The Nicaragua convergent margin: seismic reflection imaging of the source of a tsunami earthquake. In: Dixon, T., Moore, J. (Eds.), The Seismogenic Zone of Subduction Thrust Faults. Columbia University Press, New York, pp. 257–287.

Meschede, M., Zweigel, P., Kiefer, E., 1999. Subsidence and extension at a convergent plate margin: evidence for subduction erosion of Costa Rica. Terra Nova 11, 112–117.

Mitchell, N.C., 1993. A model for attenuation of backscatter due to sediment accumulations and its application to determine sediment thickness with GLORIA sidescan sonar. Journal of Geophysical Research 98 (B12), 22477–22493.

Moerz, T., Fekete, N., Kopf, A., Brueckmann, W., Kreiter, S., Huenerbach, V., Masson, D., Hepp, D.A., Schmidt, M., Kutterolf, S., Sahling, H., Abegg, F., Spiess, V., Suess, E., Ranero, C.R., 2005. Styles and productivity of mud diapirism along the Middle American margin, part ii: mound Culebra and mounds 11, and 12. In: Martinelli, G., Panahi, B. (Eds.), Mud Volcanoes, Geodynamics and Seismicity. NATO Science Series, vol. IV. Springer, Dordrecht, pp. 49–76.

Obzhirov, A.I., Kazanskiy, B.A., Melnichenko, Y.I., 1989. Effects of sound dispersion within the near-bottom waters of marginal parts of the Okhotsk Sea. Tikhookeanskaya Geologiya (Russian Journal of Pacific Geology) 2, 119–121 (in Russian with English abstr).

Orange, D.L., Jun, J., Maher, N., Barry, J., Greene, G., 2002. Tracking California seafloor seeps with bathymetry, backscatter and ROVs. Continental Shelf Research 22, 2273–2290.

Parker, G., 1982. Conditions for the ignition of catastrophically erosive turbidity currents. Marine Geology 46, 307–327.

Paull, C.K., Hecker, B., Commeau, R., Freeman-Lynde, R.P., Neumann, C., Corso, W.P., Golubic, S., Hook, J.E., Sikes, E., Curray, J., 1984. Biological communities at the Florida escarpment resemble hydrothermal vent taxa. Science 226, 965–967.

Pecher, I.A., Ranero, C.R., von Huene, R., Minshull, T.A., Singh, S.C., 1998. The nature and distribution of bottom simulating reflectors at the Costa Rican convergent margin. Geophysical Journal International 133, 219–229.

Petersen, C.J., Klaucke, I., Weinrebe, W., Ranero, C.R., 2009. Fluid seepage and mound formation offshore Costa Rica revealed by deep-towed sidescan sonar and subbottom profiler data. Marine Geology 266, 172–181.

Ranero, C.R., von Huene, R., 2000. Subduction erosion along the Middle America convergent margin. Nature 404, 748–752.

Ranero, C.R., von Huene, R., Flueh, E., Duarte, M., Baca, D., McIntosh, K., 2000. A cross section of the convergent Pacific margin of Nicaragua. Tectonics 19 (2), 335–357.

Ranero, C.R., Phipps Morgan, J., McIntosh, K., Reichert, C., 2003. Bending related faulting and mantle serpentinization at the Middle America trench. Nature 425, 367–373.

Sager, W.W., MacDonald, I.R., Hou, R., 2003. Geophysical signatures of mud mounds at hydrocarbon seeps on the Louisiana continental slope, northern Gulf of Mexico. Marine Geology 198, 97–132.

Sager, W.W., MacDonald, I.R., Hou, R., 2004. Sidescan sonar imaging of hydrocarbon seeps on the Louisiana continental slope. AAPG Bulletin 88, 725–746.

Sahling, H., Rickert, D., Lee, R.W., Linke, P., Suess, E., 2002. Macrofaunal community structure and sulfide flux at gas hydrate deposits from the Cascadia convergent margin. Marine Ecology Progress Series 231, 121–138.

Sahling, H., Masson, D.G., Ranero, C.R., Hühnerbach, V., Weinrebe, W., Klaucke, I., Bürk, D., Brückmann, W., Suess, E., 2008a. Fluid seepage at the continental margin offshore Costa Rica and southern Nicaragua. Geochemistry Geophysics Geosystems 9, 5. doi:10.1029/2008GC001978.

Sahling, H., Bohrmann, G., Spiess, V., Bialas, J., Breitzke, M., Ivanov, M., Kasten, S., Krastel, S., Schneider, R., 2008b. Pockmarks in the Northern Congo Fan area, SW Africa: complex seafloor features shaped by fluid flow. Marine Geology 249, 206–225.

Shipley, T.H., Stoffa, P.L., Dean, D.F., 1990. Underthrust sediments, fluid migration paths, and mud volcanoes associated with the accretionary wedge off Costa Rica: Middle America trench. Journal of Geophysical Research 95, 8743–8752.

Sibuet, M., Olu, K., 1998. Biogeography, biodiversity and fluid dependence of deep-sea cold-seep communities at active and passive margins. Deep-Sea Research Part II 45, 517–567.

Stockwell Jr., J.W., 1999. The CWP/SU: seismic Un*x Package. Computers and Geosciences 25 (4), 415–419.

Talukder, A.R., Bialas, J., Klaeschen, D., Buerk, D., Brueckmann, W., Reston, T., Breitzke, M., 2007. High-resolution, deep tow, multichannel seismic and sidescan sonar survey of the submarine mounds and associated BSR off Nicaragua pacific margin. Marine Geology 241, 33–43.

Talukder, A.R., Bialas, J., Klaeschen, D., Brueckmann, W., Reston, T., Petersen, J., 2008. Tectonic framework of the mud mounds, associated BSRs and submarine landslides, offshore Nicaragua Pacific margin. Journal of the Geological Society, London 165, 167–176.

Teichert, B.M.A., Eisenhauer, A., Bohrmann, G., Haase-Schramm, A., Bock, B., Linke, P., 2003. U/Th Systematics and ages of authigenic carbonates from Hydrate Ridge, Cascadia Margin: recorders of fluid flow variations. Geochimica et Cosmochimica Acta 67, 3845–3857.

Torres, M.E., McManus, J., Hammond, D.E., de Angelis, M.A., Heeschen, K.U., Colbert, S.L., Tryon, M.D., Brown, K.M., Suess, E., 2002. Fluid and chemical fluxes in and out of sediments hosting methane hydrate deposits on Hydrate Ridge, OR, I: Hydrological provinces. Earth and Planetary Science Letters 201, 525–540.

von Huene, R., Ranero, C.R., Weinrebe, W., Hinz, K., 2000. Quaternary convergent margin tectonics of Costa Rica, segmentation of the Cocos Plate, and Central American volcanism. Tectonics 19 (2), 314–334.

von Huene, R., Ranero, C.R., Vannucchi, P., 2004. Generic model of subduction erosion. Geology 32 (10), 913–916.

Walther, C.H.E., Flueh, E.R., Ranero, C.R., von Huene, R., Strauch, W., 2000. Crustal structure across the Pacific margin of Nicaragua: evidence for ophiolitic basement and a shallow mantle sliver. Geophysical Journal International 141, 759–777.